Multiple Sclerosis and Related Disorders 107 (2026) 107012

Contents lists available at ScienceDirect

Multiple Sclerosis and Related Disorders

journal homepage: www.elsevier.com/locate/msard

Real-world detection of paramagnetic rim lesions and their association with disease burden in multiple sclerosis

Olavi Misin [a,b,c,d], Anni Piispanen [c], Markus Matilainen [a,b,c,d], Riitta Parkkola [e], Mikko Nyman [e], Teija Sainio [f], Jussi Hirvonen [e], Laura Airas [a,b,c,d,*]

[a] Turku PET Centre, Turku University Hospital, University of Turku, and Åbo Akademi University, Turku, Finland
[b] Neurocenter, Turku University Hospital, Turku, Finland
[c] Clinical Neurosciences, University of Turku, Turku, Finland
[d] InFLAMES Research Flagship, University of Turku, Turku, Finland
[e] Department of Radiology, Turku University Hospital, University of Turku, Turku, Finland
[f] Department of Medical Physics, Turku University Hospital, University of Turku, Turku, Finland

ARTICLE INFO

Keywords:
Paramagnetic rim lesions
Multiple Sclerosis
Susceptibility weighted imaging

ABSTRACT

Background: Paramagnetic rim lesions (PRLs) are an emerging MRI biomarker in multiple sclerosis (MS). On susceptibility-sensitive MRI, PRLs are characterized by a paramagnetic shift at the lesion rim corresponding to iron-laden macrophages and microglia, and PRL detection can hence be viewed as a proxy for lesion-associated smoldering inflammation in MS brain. The aim of this study was to identify PRLs in a standard university hospital setting to explore the associations between PRL burden and MS-related clinical and paraclinical parameters.
Methods: We retrospectively reviewed all 3T brain MRI studies performed as part of MS patient management at a tertiary university hospital in Finland between September 2021 and December 2023. PRLs were visually identified on filtered phase images from susceptibility-weighted imaging (SWI) sequences. Brain volumetric data were extracted from post-contrast 3D T1-weighted images using an automated quantification tool (cNeuro® cMRI). Clinical and laboratory variables were obtained by manual chart review from electronic medical records.
Results: The final cohort included 206 patients. 34% of patients had at least one PRL (the PRL1+ group). The median number of PRLs in the PRL1+ group was 2 and the maximum number was 11. Within the PRL1+ group, PRL count correlated positively with Expanded Disability Status Scale (EDSS), Multiple Sclerosis Severity Score (MSSS) and T2 lesion volume. Patients with PRLs had significantly smaller thalami compared to those without PRLs.
Discussion: Our real-world data reinforce evidence that PRLs are linked to more severe disease and demonstrate that PRL identification using manufacturer-reconstructed SWI filtered phase images provides a feasible imaging parameter to assess progression-associated pathology in MS in a standard clinical setting.

1. Introduction

Paramagnetic rim lesions (PRLs) are an emerging MRI biomarker of multiple sclerosis (MS) representing chronic, low-grade intraparenchymal brain inflammation. (Absinta et al., 2021) Histopathologically, the paramagnetic rims correspond to iron-laden phagocytes at the border of chronic active MS lesions. (Kuhlmann et al., 2017) PRLs are highly specific for MS, (Maggi et al., 2020; Hemond et al., 2025) are associated with greater neurological disability, (Absinta et al., 2019) and predict later disease progression. (Reeves et al., 2024) The seminal studies describing PRLs were performed in high-level research institutes using research-dedicated MRI scanners. (Dal-Bianco et al., 2017; Absinta et al., 2016) The significance of the utilization of this biomarker in clinical practice was recently solidified as PRLs were included in the 2024 revisions of the McDonald diagnostic criteria for MS. (Montalban et al., 2025) Furthermore, being an imaging proxy for lesion-associated smoldering inflammation, PRL detection may have significance in determining who benefits best from microglia-targeting progression-slowing treatments, such as BTK inhibitors. (Oh et al., 2025) These developments accentuate the need to detect PRLs reliably and practically for MS diagnostics and care in standard clinical settings.

To explore the PRL-detection achievability in a clinical setting, we

* Corresponding author at: Turku PET Centre, Turku University Hospital, University of Turku, and Åbo Akademi University, Turku, Finland.
E-mail address: laura.airas@utu.fi (L. Airas).

https://doi.org/10.1016/j.msard.2026.107012
Received 14 January 2026; Accepted 15 January 2026
Available online 16 January 2026

identified PRLs in routine 3T MRI images obtained for MS diagnostics and/or follow-up of the patients using manufacturer-reconstructed SWI filtered phase images. We explored the associations between PRL burden and patients' clinical and paraclinical parameters.

2. Materials and methods

2.1. Patients

We retrospectively screened all brain MRI studies that were performed using our routine MS-protocol in Turku University Hospital (Tyks) between 1.9.2021 and 31.12.2023. We only included 3T scans with a 3D SWI-sequence, and patients with clinically definite MS. Exclusion criteria were neurological diseases other than MS, age under 18 years, and insufficient MRI data. Three separate MRI scanners were eligible, but one was excluded, as it provided only 5 patients in total. In case of multiple eligible scans from one patient, the earliest one was chosen.

Clinical data were obtained by manual chart review from electronic medical records. This data included neurological disability ratings (Expanded Disability Status Scale, EDSS), disease subtype, diagnosis date of MS, onset date of MS symptoms, data from the diagnostic lumbar puncture (total protein concentration, IgG-Index and number of oligoclonal bands), number of enhancing T1 lesions on the diagnostic MRI, and disease-modifying therapy use. EDSS, disease subtype, and class of disease-modifying therapy were recorded at the time of the MR imaging for PRLs. The presence of enhancing lesions on T1-weighted images on diagnostic MRI was based on the original radiological report.

2.2. Image acquisition

The final cohort included two different 3T MRI scanners: Signa Premier, General Electric Healthcare (Wisconsin, USA), and Magnetom Skyra Fit, Siemens Healthineers (Erlangen, Germany). The scanners had 84 and 122 patients, respectively. 21-channel and 20-channel head and neck coils were used, respectively. SWIs were generated automatically by the scanner software provided by the manufacturer. A consistent acquisition protocol for MS patients were used with both scanners. The exact imaging parameters can be found in supplementary Tables 1 and 2.

2.3. Image analysis

Manufacturer-reconstructed SWI filtered phase images and FLAIR images were examined side by side using the Philips Vue PACS (Picture Archiving and Communication System) deployed at Turku University Hospital. Paramagnetic rim lesions were identified on filtered phase images by an experienced rater (OM) blinded to clinical data. The recent North American Imaging in MS Cooperative (NAIMS) consensus criteria (Bagnato et al., 2024) were used in defining a PRL. A conservative approach was used with ambiguous cases, defining them as negative for PRL.

2.4. Quantitative MRI analysis

Brain parenchymal volume, cortical volume, ventricular volume and deep gray matter volumes were extracted from post-contrast 3D T1 MR images and white matter lesion volumes were extracted from 3D FLAIR MR images using cNeuro® cMRI quantification tool (Combinostics Ltd, Tampere, Finland). (Lötjönen et al., 2010; Koikkalainen et al., 2016) All volumes were normalized for age, sex, and head size. The cNeuro® tool is CE marked and is in clinical use at Turku University Hospital.

2.5. Statistical analyses

Statistical analyses were conducted using R (version 4.5.0). All tests were two-tailed and a p-value < 0.05 was considered significant in all analyses. As most of the data was non-normally distributed, non-parametric statistics were used in basic analyses. Group comparisons were done with Wilcoxon signed-rank test and correlational analyses were conducted using the Spearman rank correlations. Contingency tables were tested with Fisher's exact test for class variables.

To adjust the comparisons for disease duration, all analyses were further modelled using linear (continuous outcomes), logistic (binary outcomes) or ordinal (ordinal outcomes) regression. If the model assumptions were not fulfilled (using e.g. Shapiro-Wilk's normality test of residuals, Cook's distance or QQ plot, and specifically in ordinal regression proportional odds assumption), variable transformations were used. These included log(EDSS+2) as the EDSS outcome, log(volume +1) as the ventricular and T2 lesion volume outcomes, or square root or power of two transformation of the disease duration. If the transformations were not enough, the results were confirmed using a removal of an outlier as the sensitivity analysis, or a robust regression.

A forward-type stepwise linear regression model was constructed to explore the best variables predicting EDSS values. PRL count, T2 lesion volume, brain parenchymal volume, ventricular volume, thalamic volume and age were considered as potential predictors. The model building began with a model without any variables, and in each step, the most suitable of the aforementioned variables according to the Akaike Information Criterion (AIC) was added to the model. This was continued until no additional variable improved the model. After the final model with the lowest AIC value was established, the model was checked for its assumptions (e.g., linearity of the residuals, multicollinearity and influential values).

To examine whether the relationship between PRL group and age varies by scanner type, age was modeled as a function of PRL group, scanner type, and their interaction using ANOVA.

3. Results

3.1. Clinical and laboratory associations with PRL-presence

Characteristics of the study population are summarized in Table 1. A total of 206 MS patients were included in the final cohort. The overall patient-level prevalence of PRLs was 34%. Among patients with at least one PRL (the PRL1+ group) the median number of PRLs was 2 and the maximum number was 11. Patients in the PRL1+ group were significantly younger and had a shorter disease duration (Table 1 and Fig. 1) compared to patients with no PRLs (the PRL0 group). The PRL1+ group had somewhat fewer females, 64% vs. 77%, but this difference was not statistically significant. Representative examples of PRL findings for the two MRI scanners are shown in Fig. 2.

PRL1+ and PRL0 groups did not differ significantly in terms of disease subtype (relapsing remitting vs progressive), class of disease-modifying therapy or the presence of enhancing T1 lesions at the time of MS diagnosis. Likewise, the PRL groups did not differ significantly in terms of EDSS or MSSS, even when adjusting for disease duration.

Data on cerebrospinal fluid (CSF) at MS diagnosis were available for 168 patients (Table 1). PRL1+ and PRL0 groups did not differ significantly in terms of CSF total protein content, IgG index, or rates of positive oligoclonality defined as $\geq$ 2 oligoclonal bands. There was considerable variation in time between the CSF analysis and the studied MRI. The PRL1+ group had significantly shorter disease durations.

3.2. Quantitative MRI associations with PRL-presence

The PRL1+ group had significantly lower thalamic volumes compared to patients negative for PRLs (Table 1). When adjusting for disease duration, the differences in brain parenchymal volume, ventricular volume, and T2 lesion volume also became significant (Table 1).

Data on T1-enchancing lesions at MS diagnosis were available for 150 patients. The PRL1+ group had somewhat more enhancing lesions, 47% vs. 30%, but this difference was not significant, and adjusting for

Table 1
Summarized demographic, clinical, laboratory, and MRI characteristics of the cohort. P-values were adjusted for disease duration. All MRI volumes are normalized values. MRI scanner 1: Siemens Magnetom Skyra Fit. MRI scanner 2: GE Signa Premier.

	Whole cohort	PRL 0	PRL 1+	p-value	p-value, adjusted
Demographic and clinical data					
N (% total)	206	136 (66)	70 (34)		
Age, years, mean ± SD	45 ± 12	47 ± 12	42 ± 10	**<0.001**	
Disease duration, years, mean ± SD	13 ± 9.5	15 ± 10	10 ± 7.3	**<0.001**	
Sex, female, No. (%)	150 (73)	105 (77)	45 (64)	0.068	0.11[a]
RRMS / PMS, No.	186 / 20	121 / 15	65 / 5	0.46	0.92[a]
EDSS, median (IQR)	2.0 (1.0 - 3.5)	2.0 (1.0 - 3.5)	2.0 (1.1 - 3.0)	0.44	0.37[b,e]
MSSS, median (IQR)	2.3 (1.0 - 3.9)	2.1 (1.0 - 3.8)	2.9 (1.0 - 4.1)	0.21	-
High efficacy DMT, No. (%)	107 (52)	71 (52)	36 (51)	1	0.47[c]
Moderate efficacy DMT, No. (%)	73 (35)	48 (35)	25 (36)		
No DMT at assesment, No. (%)	26 (13)	17 (13)	9 (13)		
CSF at MS diagnosis					
CSF data available, No. (%)	168 (82)	110 (81)	58 (83)	0.85	
Time between CSF and MRI, years, mean ± SD	9.9 ± 7.1	11 ± 7.4	8.0 ± 6.1	**0.028**	-
Total protein, mg/L, mean ± SD	379 ± 146	381 ± 143	375 ± 154	0.33	0.94[b,f]
IgG index, mean ± SD	1.0 ± 0.57	1.0 ± 0.57	1.1 ± 0.58	0.12	0.17[b,f]
Oligoclonal bands ≥ 2, No. (%)	141 (84)	89 (81)	52 (90)	0.36	0.81[a,g]
T1C+ lesions at MS diagnosis					
T1C+ data available, No. (%)	150 (73)	99 (73)	51 (73)	1	
Gadolinium-enhancing lesions ≥ 1 at MS diagnosis, No. (%)	54 (36)	30 (30)	24 (47)	**0.050**	0.11[a,h]
MRI volumes					
MRI scanner, 1 vs 2, No. (%)	122 / 84	81 / 55	41 / 29	1	
Brain parenchymal volume, mean ± SD	1096 ± 49	1101 ± 46	1088 ± 53	0.10	**0.0048**[b,i]
Cortical volume, mL, mean ± SD	539 ± 23	540 ± 24	537 ± 23	0.28	0.083[d]
Ventricular volume, mL, mean ± SD	50 ± 24	48 ± 22	54 ± 28	0.16	**0.032**[b,j]
Thalamic volume, mL, mean ± SD	14 ± 1.5	15 ± 1.4	14 ± 1.7	**0.048**	**0.001**[b,k]
T2 lesion volume, mL, mean ± SD	9.3 ± 11	9.1 ± 12	9.8 ± 9.3	0.094	**0.001**[b,j,k]

PRL: paramagnetic rim lesions; RRMS: relapsing remitting multiple sclerosis; PMS: progressive multiple sclerosis; EDSS: Expanded Disability Status Scale; MSSS: Multiple Sclerosis Severity Score; DMT: disease modifying treatment; CSF: cerebrospinal fluid; MRI: magnetic resonance imaging. High efficacy DMT: anti-CD20 monoclonal antibodies, natalizumab, alemtuzumab, caldribine or fingolimod. Moderarate efficacy DMT: any other DMT.
Unadjusted p-values are from Welch's t-test (variables with mean ± SD), Wilcoxon rank-sum test (variables with median, IQR) or Fisher's exact test (variables with counts and proportions).
a) p-value from logistic regression, b) p-value from linear regression, c) p-value from ordinal regression, d) p-value from robust linear regression, e) log(edss+ 2) as an outcome, f) non-significance confirmed with robust regression g) square root of disease duration as the adjusting variable, h) disease duration squared as the adjusting variable, i) significance confirmed using robust linear regression, j) log(volume +1) as an outcome, k) significance confirmed with sensitivity analysis (removal of an outlier).

disease duration further diluted the difference.

PRL groups showed a similar lesion distribution between MRI scanners. Likewise, age distributions in PRL groups did not depend on the MRI scanner (ANOVA, p-value of the interaction 0.40).

3.3. Clinical and quantitative MRI associations with PRL-number

Among PRL-positive patients, PRL count correlated positively with EDSS, MSSS and T2 lesion volume (Table 2 and Fig. 3). Negative correlations were seen with brain parenchymal volume and thalamic volume. We sought to explore these correlations further using a stepwise linear regression model with EDSS as the outcome. PRL count, T2 lesion volume, brain parenchymal volume, ventricular volume, thalamic volume and age were considered as potential predictors. All parameters except thalamic and ventricular volumes remained in the final model (Supplementary Table 3). While PRL count was not the strongest predictor, it improved the model significantly.

When exploring the results using three PRL-groups (0, 1-3 and 4+) (Maggi et al., 2020; Absinta et al., 2019), it was noted that 52 patients (25%) had 1-3 PRLs and 18 patients (9%) had 4+ PRLs (Supplementary Table 4). The PRL4+ group had significantly higher EDSS and significantly lower thalamic and brain parenchymal volumes (Fig. 4).

4. Discussion

Our study demonstrates the feasibility of PRL detection in a standard university hospital setting. We used 3T MRI scans obtained during routine diagnostic evaluation or follow-up of MS patients at our clinic. The PRLs were visually identified on filtered phase images from susceptibility-weighted imaging (SWI) sequences which were generated automatically by the scanner software provided by the manufacturer. Importantly, our cohort of 206 patients with clinically definite MS of variable severities and disease durations provides a robust sample for a retrospective analysis.

PRLs are highly specific for MS and if detected, can improve diagnostic accuracy. (Maggi et al., 2020; Hemond et al., 2025) Hence, PRL detection was recently incorporated into the MS diagnostic criteria, which increases the importance of their straighforward detection in a standard clinical setting. (Montalban et al., 2025) Furthermore, PRLs can contribute to the assessment of the presence of smoldering inflammation in MS brain. This has increasing significance in the advent of the availability of smoldering inflammation-reducing treatments aiming to slow down MS disease progression. (Oh et al., 2025) The prognostic value of PRLs for later disease progression has been firmly established (Reeves et al., 2024; Blindenbacher et al., 2020; Cagol et al., 2024; Altokhis et al., 2022) and correlations between PRL count and EDSS in a cross-sectional setting have been reported. (Liu et al., 2025; Skattebøl et al., 2025) We found no difference in EDSS or MSSS between the PRL1+ and PRL0 groups, but we did observe positive correlations between EDSS and MSSS scores with the PRL counts among the PRL1+ group. PRLs have been extensively linked with higher gray matter atrophy and higher T2 lesion volume. (Reeves et al., 2024; Kazimuddin et al., 2025; Reeves et al., 2024) Similarly, our patients with PRLs had higher T2 lesion loads and lower volumes of thalamus and whole brain parenchyma.

Recent evidence suggests that PRLs represent a relatively early feature of lesion evolution (Klistorner et al., 2025) and they may fade away slowly with age. (Absinta et al., 2021; Dal-Bianco et al., 2021) This highlights the importance of early susceptibility-sensitive imaging in MS, as early imaging maximizes PRL detection and enables timely therapeutic intervention for aggressive or progressive MS disease.

Gadolinium-enhancing T1 lesions at MS diagnosis, similar to the CSF

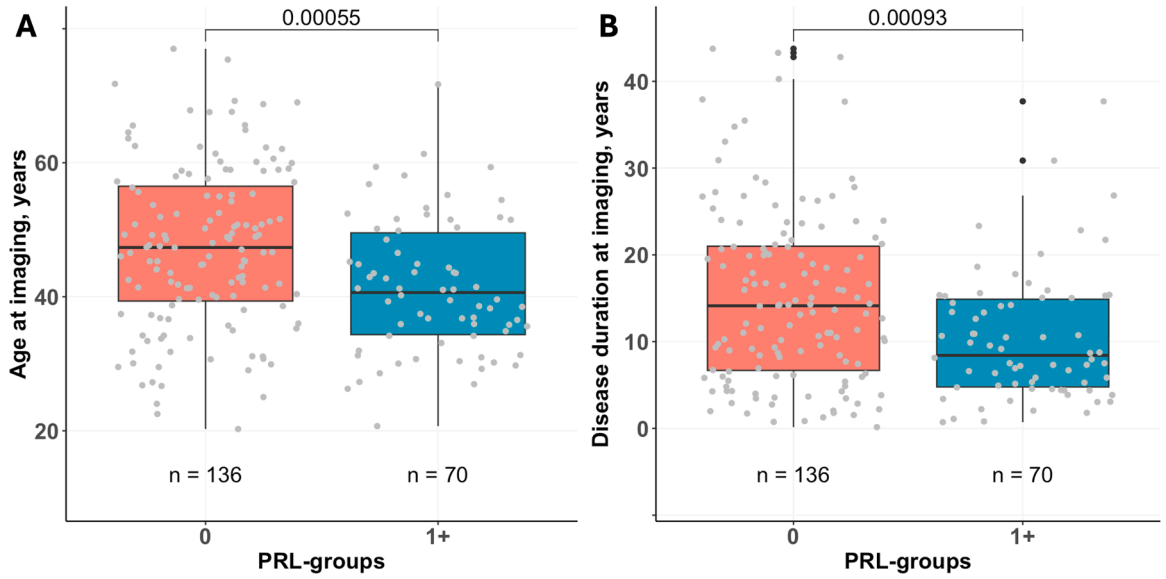

Fig. 1. Box plots depicting age and disease duration between the PRL groups. Patients with ≥ 1 PRLs were significantly younger and had a significantly shorter disease duration (A & B).

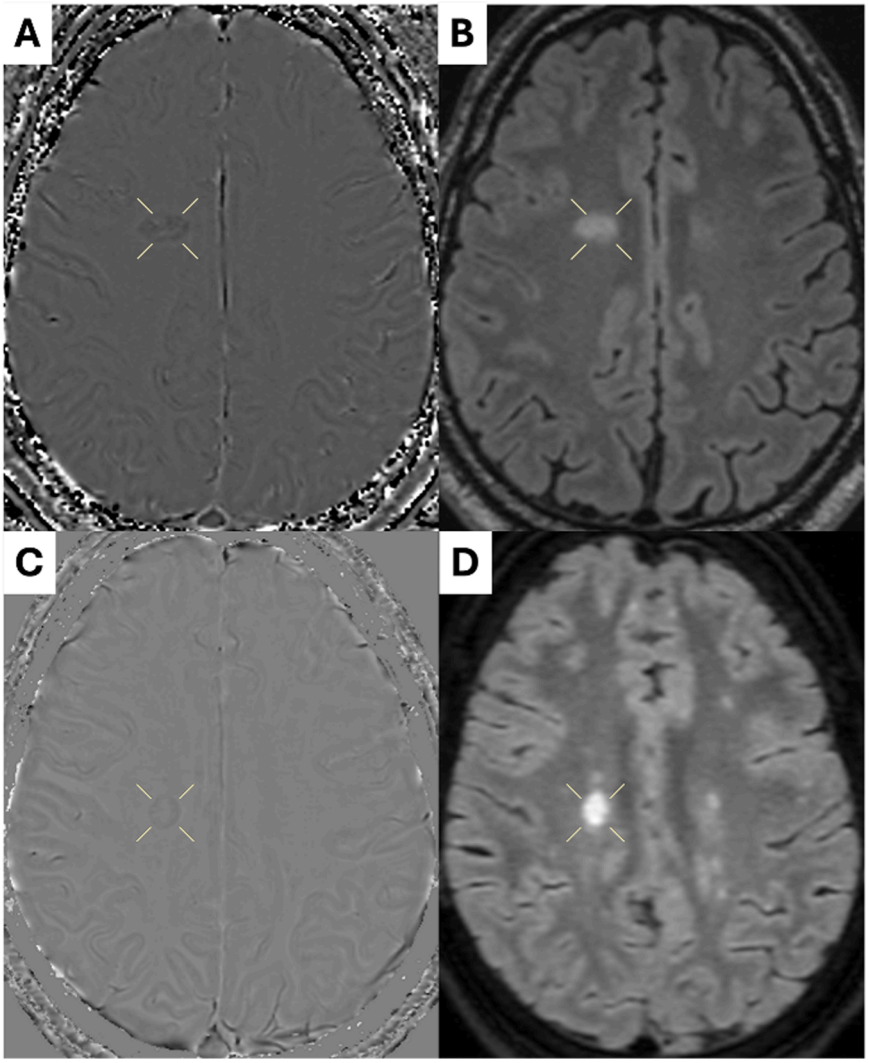

Fig. 2. PRL findings from the two MRI scanners in the cohort. A & B: a PRL on filtered phase (A) and FLAIR (B) images from MRI scanner 1 (Siemens Magnetom Skyra Fit). C & D: a PRL on filtered phase (C) and FLAIR (D) images from MRI scanner 2 (GE Signa Premier).

Table 2
Correlations of PRL count with clinical and radiological parameters among PRL-positive patients (n = 70).

	Spearman's ρ	95% CI	p-value
Demographic and clinical data			
Age	0.026	-0.21 – 0.26	0.83
Disease duration	0.18	-0.053 – 0.40	0.13
EDSS	0.31	0.075 – 0.50	**0.010**
MSSS	0.24	0.002 – 0.45	**0.048**
CSF at MS diagnosis			
Total protein, mg/L, mean ± SD	0.079	-0.20 – 0.34	0.57
IgG index, mean ± SD	0.088	-0.17 – 0.34	0.51
MRI volumes			
Brain parenchymal volume	-0.37	-0.56 - -0.15	**0.001**
Cortical volume	-0.14	-0.36 – 0.10	0.26
Ventricular volume	0.22	-0.02 – 0.43	0.073
Thalamic volume	-0.52	-0.67 - -0.32	**<0.001**
T2 lesion volume	0.54	0.35 – 0.69	**<0.001**

PRL: paramagnetic rim lesions; EDSS: Expanded Disability Status Scale; MSSS: Multiple Sclerosis Severity Score; CSF: cerebrospinal fluid; MRI: magnetic resonance imaging.

albumin quotient, reflect increased blood-brain barrier permeability at disease onset. (Uher et al., 2016; Gaitán et al., 2011) Approximately 18-44% of gadolinium-enhancing lesions develop a paramagnetic rim (Zhang et al., 2019; Wenzel et al., 2022; Al Gburi et al., 2025) and key predictors for this conversion include larger intial enhancing lesion size and a centripetal enhancement pattern. (Al Gburi et al., 2025; Absinta et al., 2013) Our patiens with PRLs were somewhat more likely to have enhancing lesions at MS diagnosis, but adjustment for disease duration at the time of PRL detection abrogated this difference. In a similar setting, Wittayer et al. also found no significant differences in initial enhancement rates between PRL groups. (Wittayer et al., 2023) Similarly, we did not observe an increased CSF albumin quotient (Hemond et al., 2022) or on increased total CSF protein concentration (Wittayer et al., 2023; Hemond et al., 2022) at the time of diagnosis among the PRL1+ cohort. This may be explained by the wide variation in the interval between lumbar puncture and PRL assessment in our data set (9.9 ± 7.1 years, mean ± SD).

The Turku University Hospital serves a catchment area of a population of 500 000 and our basic MS care represents well any functions carried out at a standard tertiary MS center. (Marrie et al., 2022) Being an academic hospital in a geographic area of high MS prevalence, our hospital has however taken several extra measures to improve the quality of MS diagnostics and MS care. These measures are run solely by hospital employee-based operations in the neurology department and radiology department and are covered financially by hospital management. An MS register was integrated to the electronic patient record system in year 2014 with yearly recording of EDSS scores and real-time recording of MS-related therapies. (Ahvenjärvi et al., 2025) Quantitative evaluation of MRI images obtained for diagnostics and follow-up of MS patients in the clinic was enabled in 2020 following collaboration with Combinostics, Tampere, Finland, a company providing an automated quantification tool for brain volumetric data for all MS patients treated at our hospital. (Lötjönen et al., 2010) Finally, since September 2021 SWI sequences have been included in the MRI acquisition protocol for MS diagnostics and follow-up. Various susceptibility-sensitive sequences can be used for PRL detection (Martire et al., 2022), but none of them are as established and widely used in clinical practice as SWI. (Rubin et al., 2022) These follow-up elements provide valuable real-world quantitative data for clinical and radiological evaluation of our MS patients and thus facilitate and improve the quality of their clinical and radiological follow-up.

The overall patient-level prevalence of PRLs in this study (34%) was slightly lower compared to that reported by a recent meta-analysis (41%). (Kwong et al., 2021) This may reflect the conservative approach chosen to defining a PRL and the limitations of our SWI filtered phase compared to research imaging protocols. In accordance to previous studies, we demonstrate a strong association of younger age, shorter disease duration and elements of more aggressive disease with PRL presence. (Reeves et al., 2024; Klistorner et al., 2025; Pinto et al., 2022).

5. Conclusion

Our findings support the use of manufacturer-reconstructed SWI filtered phase images for PRL identification in a clinical setting, thereby bridging the gap between research project-based PRL-detection and

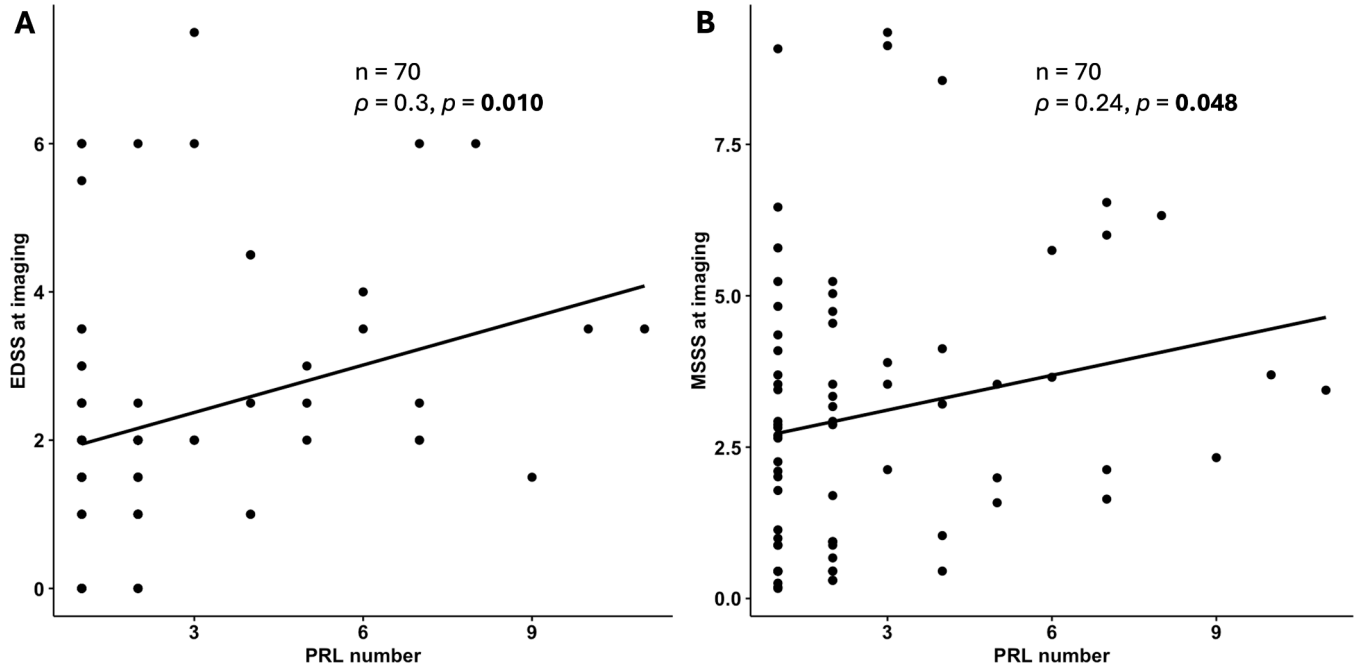

Fig. 3. Correlations of PRL count with EDSS and MSSS among PRL-positive patients. PRL: paramagnetic rim lesions; EDSS: Expanded Disability Status Scale; MSSS: Multiple Sclerosis Severity Score.

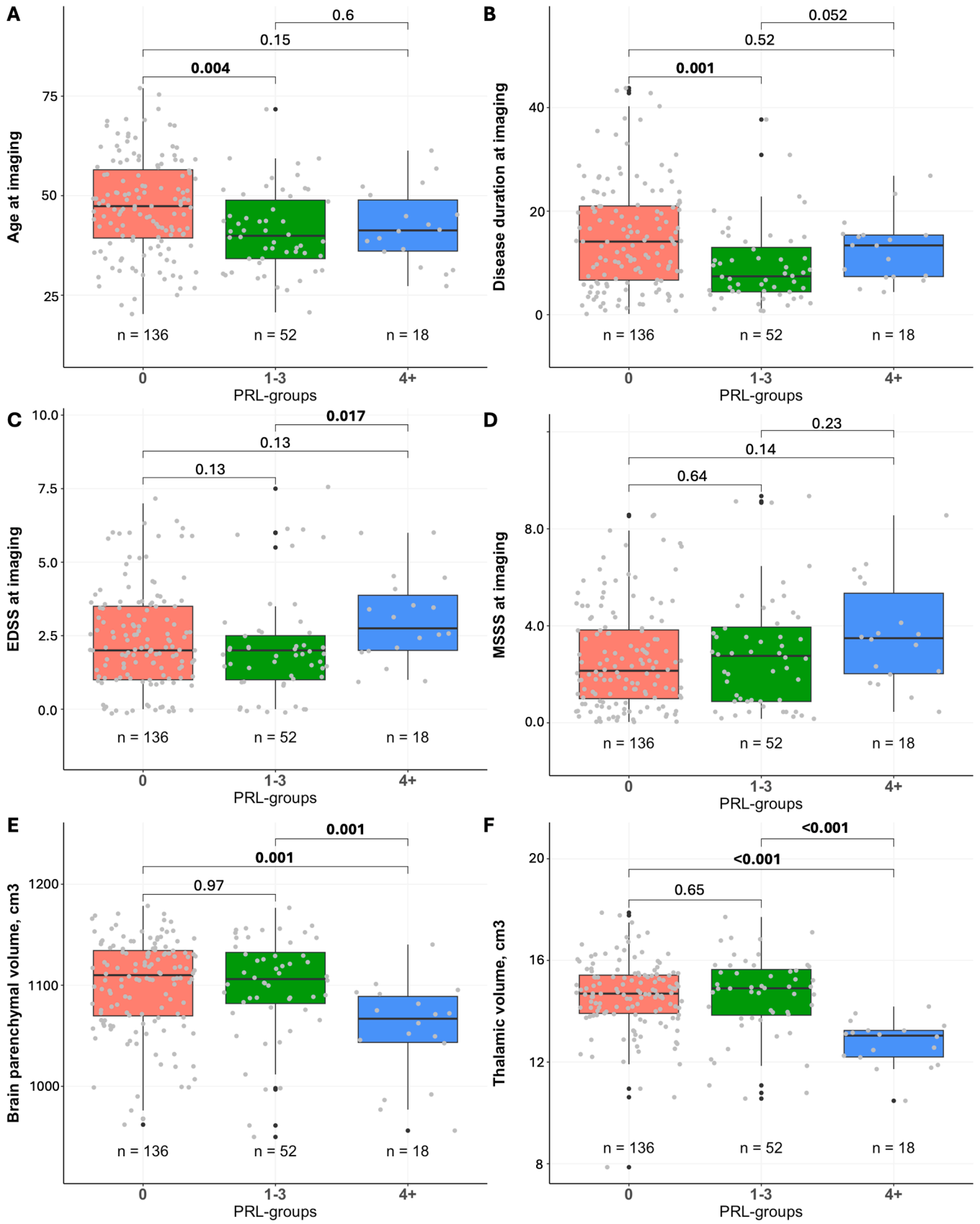

Fig. 4. Box plots depicting clinical and radiological parameters between three PRL groups. Patients with 4+ PRLs had significantly higher EDSS (C) and significantly lower volumes of brain parenchyma (E) and thalamus (F). P-values are adjusted using Holm multiple comparison correction.

everyday clinical practice. Our results corroborate previous evidence linking PRLs with more aggressive clinical and radiological features, as well as their higher prevalence in early MS. PRLs represent a chronic lesion-associated manifestation of smoldering inflammation, and their detection in the clinical setting may prove highly valuable for individualized treatment efforts targeting smoldering inflammation with the aim to slow down MS progression.

Ethics statement

This study was reviewed and approved by the ethics committee of Wellbeing Services County of Southwest Finland. Patient consent was waived by our institutional review board due to the retrospective nature of the study and the lack of patient interaction.

Role of funding source

This research was supported by the Research Council of Finland's Flagship InFLAMES. The funding decision numbers are 337530, 357910 and 358823. This study was also partly supported by the Finnish Cultural Foundation and the State Research Funding (SRF) for university-level health research, Turku University Hospital, Wellbeing Services County of Southwest Finland.

CRediT authorship contribution statement

Olavi Misin: Data curation, Investigation, Visualization, Writing – original draft. **Anni Piispanen:** Data curation, Investigation. **Markus Matilainen:** Formal analysis. **Riitta Parkkola:** Supervision. **Mikko Nyman:** Resources. **Teija Sainio:** Resources. **Jussi Hirvonen:** Supervision, Writing – review & editing. **Laura Airas:** Conceptualization, Writing – review & editing.

Declaration of competing interest

Authors have nothing to declare.

Supplementary materials

Supplementary material associated with this article can be found, in the online version, at doi:10.1016/j.msard.2026.107012.

Data availability

Data cannot be publicly shared because of the national legislature on the privacy of patient data.

References

Absinta, M., Maric, D., Gharagozloo, M., et al., 2021. A lymphocyte-microglia-astrocyte axis in chronic active multiple sclerosis. Nature 597 (7878), 709–714. https://doi.org/10.1038/s41586-021-03892-7.

Kuhlmann, T., Ludwin, S., Prat, A., Antel, J., Brück, W., Lassmann, H., 2017. An updated histological classification system for multiple sclerosis lesions. Acta Neuropathol. (Berl) 133 (1), 13–24. https://doi.org/10.1007/s00401-016-1653-y.

Maggi, P., Sati, P., Nair, G., et al., 2020. Paramagnetic Rim Lesions are specific to multiple sclerosis: an international multicenter 3T MRI study. Ann. Neurol. 88 (5), 1034–1042. https://doi.org/10.1002/ana.25877.

Hemond, C.C., Dundamadappa, S.K., Deshpande, M., et al., 2025. Paramagnetic rim lesions are highly specific for multiple sclerosis in real-world data. Brain Commun. 7 (3), fcaf211. https://doi.org/10.1093/braincomms/fcaf211.

Absinta, M., Sati, P., Masuzzo, F., et al., 2019. Association of chronic active multiple sclerosis lesions with disability in vivo. JAMa Neurol. 76 (12), 1474–1483. https://doi.org/10.1001/jamaneurol.2019.2399.

Reeves, J.A., Mohebbi, M., Wicks, T., et al., 2024. Paramagnetic rim lesions predict greater long-term relapse rates and clinical progression over 10 years. Mult. Scler J. 30 (4-5), 535–545. https://doi.org/10.1177/13524585241229956.

Dal-Bianco, A., Grabner, G., Kronnerwetter, C., et al., 2017. Slow expansion of multiple sclerosis iron rim lesions: pathology and 7 T magnetic resonance imaging. Acta Neuropathol. (Berl) 133 (1), 25–42. https://doi.org/10.1007/s00401-016-1636-z.

Absinta, M., Sati, P., Schindler, M., et al., 2016. Persistent 7-tesla phase rim predicts poor outcome in new multiple sclerosis patient lesions. J. Clin. Invest. 126 (7), 2597–2609. https://doi.org/10.1172/JCI86198.

Montalban, X., Lebrun-Frénay, C., Oh, J., et al., 2025. Diagnosis of multiple sclerosis: 2024 revisions of the McDonald criteria. Lancet Neurol. 24 (10), 850–865. https://doi.org/10.1016/S1474-4422(25)00270-4.

Oh J, Fox RJ, Arnold DL. LB1.1. paramagnetic rim lesions as a prognostic and predictive biomarker in the tolebrutinib phase 3 trials for disability outcomes. Presented at: 2025 ACTRIMS Forum; February 27-March 1; West Palm Beach, FL.

Bagnato, F., Sati, P., Hemond, C.C., et al., 2024. Imaging chronic active lesions in multiple sclerosis: a consensus statement. Brain J. Neurol. 147 (9), 2913–2933. https://doi.org/10.1093/BRAIN/AWAE013.

Lötjönen, J.M., Wolz, R., Koikkalainen, J.R., et al., 2010. Fast and robust multi-atlas segmentation of brain magnetic resonance images. Neuroimage 49 (3), 2352–2365. https://doi.org/10.1016/J.NEUROIMAGE.2009.10.026.

Koikkalainen, J., Rhodius-Meester, H., Tolonen, A., et al., 2016. Differential diagnosis of neurodegenerative diseases using structural MRI data. Neuroimage Clin. 11, 435–449. https://doi.org/10.1016/J.NICL.2016.02.019.

Blindenbacher, N., Brunner, E., Asseyer, S., et al., 2020. Evaluation of the "ring sign" and the "core sign" as a magnetic resonance imaging marker of disease activity and progression in clinically isolated syndrome and early multiple sclerosis. Mult. Scler. J. - Exp. Transl. Clin. 6 (1), 2055217320915480. https://doi.org/10.1177/2055217320915480.

Cagol, A., Benkert, P., Melie-Garcia, L., et al., 2024. Association of spinal cord atrophy and brain paramagnetic rim lesions with progression independent of relapse activity in people with MS. Neurology 102 (1), e207768. https://doi.org/10.1212/WNL.0000000000207768.

Altokhis, A.I., Hibbert, A.M., Allen, C.M., et al., 2022. Longitudinal clinical study of patients with iron rim lesions in multiple sclerosis. Mult. Scler Houndmills Basingstoke Engl. 28 (14), 2202–2211. https://doi.org/10.1177/13524585221114750.

Liu, X., Wang, Y., Wei, N., et al., 2025. The characteristics and influencing factors of paramagnetic rim lesions in Chinese MS patients: A 7T MRI study. Mult. Scler Houndmills Basingstoke Engl. 31 (8), 964–974. https://doi.org/10.1177/13524585251328902.

Skattebøl, L., Lundby, R., Øverås, M.H., et al., 2025. Quantitative susceptibility mapping of paramagnetic rim lesions in early multiple sclerosis: A cross-sectional study of brain age and disability. Neuroimage Rep. 5 (3), 100277. https://doi.org/10.1016/j.ynirp.2025.100277.

Kazimuddin, H.F., Wang, J., Toubasi, A.A., et al., 2025. Paramagnetic rim lesions in early multiple sclerosis: a 7 Tesla imaging study. Brain Commun. 7 (3), fcaf215. https://doi.org/10.1093/braincomms/fcaf215.

Reeves, J.A., Bartnik, A., Jakimovski, D., et al., 2024. Associations between paramagnetic rim lesion evolution and clinical and radiologic disease progression in persons with multiple sclerosis. Neurology 103 (10), e210004. https://doi.org/10.1212/WNL.0000000000210004.

Klistorner, S., Usnich, T., Clarke, M.A., et al., 2025. The presence of a paramagnetic phase rim in multiple sclerosis is linked to lesion age: An exploratory study. Mult. Scler. J. - Exp. Transl. Clin. 11 (3), 20552173251378788. https://doi.org/10.1177/20552173251378788.

Dal-Bianco, A., Grabner, G., Kronnerwetter, C., et al., 2021. Long-term evolution of multiple sclerosis iron rim lesions in 7 T MRI. Brain J. Neurol. 144 (3), 833–847. https://doi.org/10.1093/brain/awaa436.

Uher, T., Horakova, D., Tyblova, M., et al., 2016. Increased albumin quotient (QAlb) in patients after first clinical event suggestive of multiple sclerosis is associated with development of brain atrophy and greater disability 48 months later. Mult. Scler. Houndmills Basingstoke Engl. 22 (6), 770–781. https://doi.org/10.1177/1352458515601903.

Gaitán, M.I., Shea, C.D., Dphil, I.E.E., et al., 2011. Evolution of the blood-brain barrier in newly forming multiple sclerosis lesions. Ann. Neurol. 70 (1), 22–29. https://doi.org/10.1002/ana.22472.

Zhang, S., Nguyen, T.D., Hurtado Rúa, S.M., et al., 2019. Quantitative susceptibility mapping of time-dependent susceptibility changes in multiple sclerosis lesions. AJNR Am. J. Neuroradiol. 40 (6), 987–993. https://doi.org/10.3174/ajnr.A6071.

Wenzel, N., Wittayer, M., Weber, C.E., et al., 2022. MRI predictors for the conversion from contrast-enhancing to iron rim multiple sclerosis lesions. J. Neurol. 269 (8), 4414–4420. https://doi.org/10.1007/s00415-022-11082-2.

Al Gburi, M., Mazzola, M., Absinta, M., et al., 2025. Paramagnetic rim lesion formation is predicted by the initial gadolinium-enhancing lesion diameter. Mult. Scler. J. 31 (3), 263–277. https://doi.org/10.1177/13524585241310764.

Absinta, M., Sati, P., Gaitán, M.I., et al., 2013. Seven-tesla phase imaging of acute multiple sclerosis lesions: A new window into the inflammatory process. Ann. Neurol. 74 (5), 669–678. https://doi.org/10.1002/ana.23959.

Wittayer, M., Weber, C.E., Kittel, M., et al., 2023. Cerebrospinal fluid–related tissue damage in multiple sclerosis patients with iron rim lesions. Mult. Scler. J. 29 (4-5), 549–558. https://doi.org/10.1177/13524585231155639/ASSET/IMAGES/LARGE/10.1177_13524585231155639-FIG4.JPEG.

Hemond, C.C., Baek, J., Ionete, C., Reich, DS., 2022. Paramagnetic rim lesions are associated with pathogenic CSF profiles and worse clinical status in multiple sclerosis: A retrospective cross-sectional study. Mult. Scler. J. 28 (13), 2046–2056. https://doi.org/10.1177/13524585221102921/ASSET/IMAGES/LARGE/10.1177_13524585221102921-FIG3.JPEG.

Marrie, R.A., Donkers, S.J., Jichici, D., et al., 2022. Models of care in multiple sclerosis: a survey of Canadian health providers. Front. Neurol. 13. https://doi.org/10.3389/fneur.2022.904757.

Ahvenjärvi, H., Jokinen, E., Viitala, M., et al., 2025. Evolving patterns of Initial RRMS treatment in Finland (2013-2022): insights from a nationwide multiple sclerosis register. Brain Behav. 15 (2), e70326. https://doi.org/10.1002/brb3.70326.

Martire, M.S., Moiola, L., Rocca, M.A., Filippi, M., Absinta, M., 2022. What is the potential of paramagnetic rim lesions as diagnostic indicators in multiple sclerosis? Expert Rev. NeurOther 22 (10), 829–837. https://doi.org/10.1080/14737175.2022.2143265.

Rubin, A., Waszczuk, Ł., Trybek, G., Kapetanakis, S., Bladowska, J., 2022. Application of susceptibility weighted imaging (SWI) in diagnostic imaging of brain pathologies - a practical approach. Clin. Neurol. Neurosurg. 221, 107368. https://doi.org/10.1016/j.clineuro.2022.107368.

Kwong, KCNK, Mollison, D., Meijboom, R., et al., 2021. The prevalence of paramagnetic rim lesions in multiple sclerosis: A systematic review and meta-analysis. PLoS One 16 (9), e0256845. https://doi.org/10.1371/JOURNAL.PONE.0256845.

Pinto, C., Cambron, M., Dobai, A., Vanheule, E., Casselman, JW., 2022. Smoldering lesions in MS: if you like it then you should put a rim on it. Neuroradiology 64 (4), 703–714. https://doi.org/10.1007/s00234-021-02800-0.